Pergamon

Cement and Concrete Research 32 (2002) 1473–1481

CEMENT AND CONCRETE RESEARCH

Electrical conductivity and rheological properties of ordinary Portland cement–silica fume and calcium hydroxide–silica fume pastes

Th.M. Salem*

Department of Chemistry, University College for Girls, Ain Shams University, Asmaa Fahmy Street, El-Merghany Road, Heliopolis, Cairo, Egypt

Received 23 August 2001; accepted 3 April 2002

Abstract

Two groups of solids mixtures were prepared: (i) the first group includes four mixes having different ordinary Portland cement/silica fume (OPC/SF) weight ratios and (ii) the second group consists of four blends having different $Ca(OH)_2$/SF molar ratios. Electrical conductivity measurements were carried out on the pastes of the first group mixes using two initial water-to-solid (W/S) ratios of 0.55 and 0.70 by weight; while the W/S ratios used for the second group mixes were 1.00 and 1.20 by weight. The measurements were done at 25 and 45 °C for each paste during setting and hardening processes after gauging with deionized water. Rheological properties were studied at room temperature for all mixes using various W/S ratios. The results obtained indicate clearly the effect of SF and W/S ratio on the rheological properties and electrical conductivity of all pastes under investigation. The relation between the electrical conductivity and rheological properties for different mixes were discussed based on the chemical nature and physical state of the hydration products formed at early ages of hydration.

Keywords: Electrical properties; Rheology; $Ca(OH)_2$; Cement paste; Silica fume

1. Introduction

Few fundamental studies concerning the electrical conductivity of cement pastes made of various types of Portland cement and clinkers, as well as clinker minerals in the presence and absence of various admixtures have been performed. The results indicated two conductivity maxima. The intensity and position of these maxima were found to be affected by the addition of various admixtures, fineness, temperature, carbonation, etc. [1–4]. The effect of high temperature on physical, mechanical properties, and microstructure of concrete containing different amounts of silica fume (SF) were also studied; the results showed that concrete specimens made with 10% SF possess the highest compressive strength and the lowest porosity values at all temperatures [5,6]. Electrical conductivity measurements of neat cement, mortar, and concrete pastes were reported in earlier publication where the electrical conductivity can be used as indication for the setting characteristics as well as the structural changes of the hardened pastes made with and without SF [7].

The influence of SF on the rheological properties of high-performance concrete was investigated; no significant effect of the quality of SF on the rheological behavior of the cement pastes containing superplasticizers was observed [8,9]. The yield stress of Portland cement pastes was determined from its creep/recovery behavior using a constant stress rheometer; it was found that the time evolution of the measured yield stress was correlated to the induction and acceleratory periods as well as the initial setting time [10]. On the other hand, the rheological properties of three sets of clinkers with varying amounts of alkalis present in different forms were studied; the laboratory tests indicated that different alkali combinations have distinctive effects on their rheological behavior [11]. The rheology of fresh fine mortars using seven dolomite fillers differ in particle size distribution and one superplasticizer was investigated; the results showed that the increase in the dolomite fineness leads to higher yield stress and plastic viscosity, while addition of superplasticizer decreases these rheology values [12,13]. Further investigations indicate that the flow curves of a high-strength gypsum-free cement were found to be pseudo-plastic type and can be described by the Bingham model [14]. Powder for binders for high-performance concrete have been investigated using a simple flow spread test;

---

* Tel./fax: +20-2-4157-804.

0008-8846/02/$ – see front matter © 2002 Elsevier Science Ltd. All rights reserved.
PII: S0008-8846(02)00809-8

the values of yield stress and plastic viscosity from concentric cylinder tests were found to be related to the flow spread test results [15]. The role of condensed SF, superplasticizers, and mineral composition of cement on the rheology of cement pastes was also reported in the literature, which lead to the conclusion that the addition of slag to cement promoted the dilatational behavior of the paste, and SF enhanced the plastic or thixotropic behavior [16,17].

2. Experimental

Ordinary Portland cement (OPC) and condensed SF were used in this study, having Blaine surface areas of 3290 and 20×10^4 cm^2/g, respectively. The chemical oxide composition of OPC is CaO, 63.05; SiO_2, 20.25; Al_2O_3, 5.13; MgO, 2.60; Fe_2O_3, 3.39; SO_3, 2.60; (Na_2O+K_2O), 2.86; and loss on ignition, 1.42, respectively; while that of SF is SiO_2, 95.50; Al_2O_3, 0.70; Fe_2O_3, 1.90; SO_3, 0.70; and loss on ignition, 1.00, respectively. Highly pure calcium hydroxide was also used as the $Ca(OH)_2$ source.

Two groups of mixtures were prepared; the first group includes four mixes having the OPC/SF weight ratios of 90:10, 80:20, 70:30, and 50:50 and are designated as mixes Ia, Ib, Ic, and Id, respectively. The second group consists of four blends having $Ca(OH)_2$/SF molar ratios of 0.80, 1.00, 1.30, and 1.70 and are designated as mixes IIa, IIb, IIc, and IId, respectively.

For conductivity measurements, the pastes of the first group mixes were made by mixing each solid mixture with distilled water using two initial water-to-solid (W/S) ratios of 0.55 and 0.70 by weight; while the W/S ratios used for the second group mixes were 1.00 and 1.20 by weight. Mixing with deionized water was carried out for 2.5 min continuously. Each paste was then transferred into a cylindrical plastic sample holder (15 mm internal diameter) with stainless steel electrodes at both sides with 12 mm distance between them and the cell was kept in a thermostatic cabinet at 100% relative humidity during the test period. The measurement began exactly 5 min after the first contact with water and up to 24 h (during setting and hardening processes) at two constant temperatures of 25 and 45 °C.

For rheological measurements, the mixes were prepared by mixing exactly 50 g dry mixture with various proportions of distilled water. The W/S ratios used for OPC–SF blends were 0.55, 0.60, 0.70, and 0.80 by weight, while those used for $Ca(OH)_2$–SF mixtures were 0.80, 0.90, 1.00, 1.10, and 1.20 by weight at room temperature. Mixing was continued for 3 min and the paste obtained was transferred to the cell of rotating coaxial cylindrical viscometer rheotest model 2.1 MLW Germany. The testing procedure was initiated after 5 min from the moment of mixing with water. The method was based on measuring the shear stress (torque, T) along complete cycles containing the ascending and descending shear rates; the initial and final speeds were 1.70 and 243 rpm, respectively. The total time for the measurement of a complete cycle was about 5 min at room temperature. Three successive cycles were measured for each sample.

3. Results and discussion

3.1. Electrical conductivity

3.1.1. OPC–SF pastes

The electrical conductance–hydration time curves obtained for the OPC–SF mixes having the weight ratios of 90:10, 80:20, 70:30, and 50:50 and are designated as mixes Ia, Ib, Ic, and Id using an initial W/S ratio of 0.55 by weight and hydrated at two constant temperatures of 25 and 45 °C are given in Fig. (1). Evidently, the conductograms shown in Fig. (1) indicate higher conductivity values during the initial interaction stages between water and mix constituents leading to the first conductivity peak within 1 h and 1/2 h for pastes hydrated at 25 and 45 °C, respectively. The results of Fig. (1) show higher conductivity values for the blends having higher OPC contents, during the initial stage of hydration. This was followed by a sharp decrease in the conductivity values with a notable appearance of a second conductivity peak located between 4.2 and 5.2 h for the pastes hydrated at 25 °C and between 1.8 and 2.6 h for the

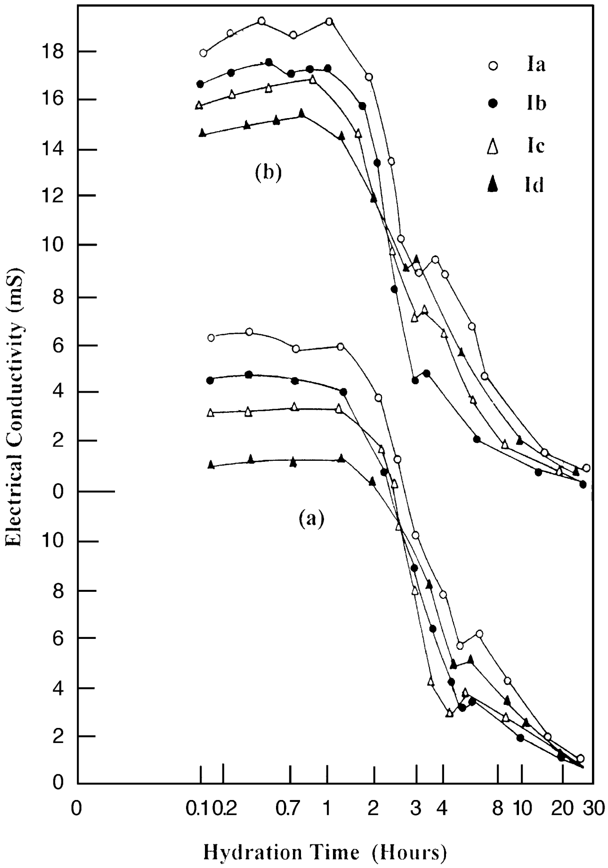

Fig. 1. Electrical conductivity–time curves of OPC–SF pastes of mixes Ia, Ib, Ic, and Id using W/S ratio of 0.55 at two temperatures (a) 25 and (b) 45 °C.

pastes hydrated at 45 °C. The second conductivity peak is shifted towards a shorter time of hydration with increasing SF content of the OPC–SF blend; similar effect was also observed with increasing hydration temperature from 25 to 45 °C.

The first conductivity maximum is a consequence of the initial hydrolysis of the OPC constituents; the charge carriers are primarily Ca^{+2}, OH^{-}, SO_4^{-2}, and alkali ions [18] and the presence of these ions might be responsible for the initial increase in the conductance values. Then, the interaction between these ions within the pore system of the paste leads to the formation of cement hydrates. These hydration products form thin insulating layers around the hydrated cement grains. These envelopes consist of electrical double layers of adsorbed calcium ions and counter ions that leads to a decrease in both of the number and mobility of ions, and consequently the conductivity values decreased after the first peak; the first peak appeared at hydration time corresponding to the predormant period [19]. The most interesting feature on the conductogram shown in Fig. (1) is the appearance of the second transient maximum on the descending section of the plot that can be explained by the ettringite–monosulfate transformation [20,21]. Alternatively, one could hypothesize protective layers around ettringite grains, which when disturbed by osmotic pressure release sulfate and other ions into the environment in a transient way. On progressive hydration, the notable consumption of the number of ions, a result of the formation and later accumulation of hydration products, is responsible for the sharp decrease in the conductivity values of the hardened blended cement pastes.

The results of Fig. (1) demonstrate also the effect of SF content on the electrical conductivity values of the blended cement pastes. It is clear that the height of the first conductivity maximum decreases as the SF content increases. This result is mainly attributed to three factors, namely (i) the decrease in the number of leaching ions during the hydration of OPC as its proportion decreases in the mixes, (ii) the degree of consumption of free $Ca(OH)_2$ released during the hydration of OPC increased as the SF content increases, and (iii) the interaction of SF with the free $Ca(OH)_2$ released as a result of OPC hydration leading to the formation of poorly crystallized calcium silicate hydrates. These effects are more pronounced during the initial stage of hydration (up to 1 h).

Evidently, the second conductivity peak is shifted towards a shorter curing time with increasing SF content of the OPC–SF blend. Therefore, the hydration interaction between SF and the free $Ca(OH)_2$ released to form C-S-H results in a decrease in the free water content of the paste leading to a sort of acceleration of the ettringite–monosulfate transformation [22].

Upon increasing the temperature to 45 °C, all the conductograms show common characteristics and are similar in shape with those obtained at 25 °C with two main differences: (i) the intensities of the conductivity maxima are higher in the conductograms obtained at 45 °C and (ii) the first and second conductivity maxima are shifted to shorter hydration times and this is associated with a sharper decrease in siemens values after each maximum. These results can be attributed to the increase of both of the degree of hydrolysis of the cement constituents and the rate of formation of hydration products upon increasing temperature. The crossing of the conductivity curves indicates that in addition to their concentration, the mobility of ions represents an important factor in affecting the conductivity values shown in Fig. (1); this result reflects the effect of the nature of pores of these samples on the mobility and therefore, on the conductivity values.

Fig. (2) shows the conductance–hydration time curves for the pastes of mixes Ia, Ib, Ic, and Id using an initial W/S ratio of 0.70 by weight and hydrated at 25 and 45 °C. It is clear that all the conductograms of Fig. (2) have almost the same shape and criteria as those of the pastes made using W/S ratio of 0.55 with two main differences, namely (i) the relatively high water content of the pastes results in an increase in the degree of initial hydrolysis of the blend as indicated by the relatively high initial conductivity values and (ii) the delayed ettringite–monosulfate transformation as a result of the relatively high W/S ratio (W/S = 0.70) leading to the appearance of the second conductivity maxima at longer time of hydration. In fact, the effects of curing

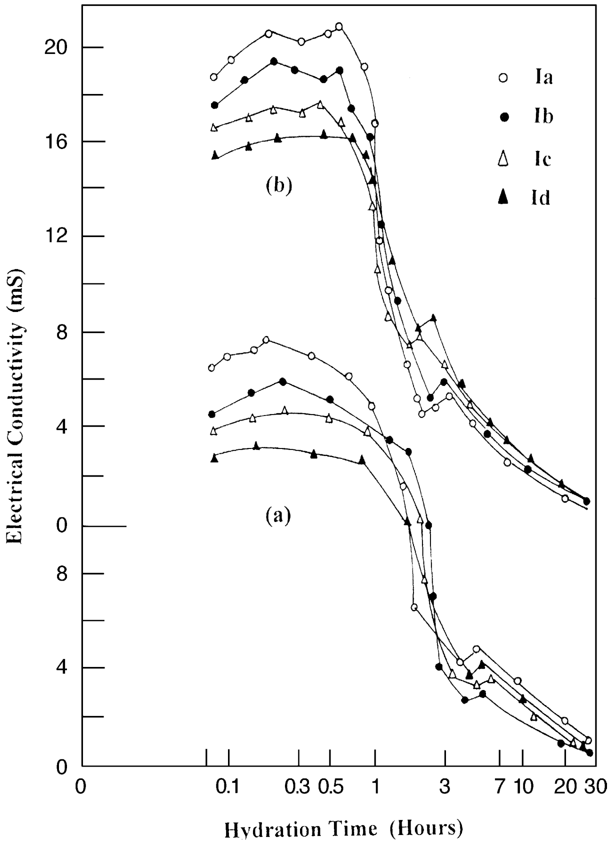

Fig. 2. Electrical conductivity–time curves of OPC–SF pastes of mixes Ia, Ib, Ic, and Id using W/S ratio of 0.70 at two temperatures (a) 25 and (b) 45 °C.

temperature and SF content on the conductograms are almost similar to that of the pastes made with W/S ratio of 0.55.

3.1.2. $Ca(OH)_2$–SF pastes

The electrical conductivity measurements were done for the $Ca(OH)_2$–SF pastes of mixes IIa, IIb, IIc, and IId having the molar $Ca(OH)_2$/SF ratios of 0.80, 1.00, 1.30, and 1.70, respectively. The conductivity–time curves are shown in Figs. (3) and (4) for the pastes made with the initial W/S ratios of 1.00 and 1.20, respectively; each paste was hydrated at two temperatures of 25 and 45 °C. Obviously, all the conductograms obtained in Figs. (3) and (4) are characterized by the appearance of one maximum. This maximum, which takes place at shorter time from the moment of mixing with water is a consequence of initial hydrolysis of calcium hydroxide, which yields Ca^{2+} and OH^- and also the sudden conversion of SF particles into a "sol" or a "gel" during the first 30 min of hydration [23]. Fig. (3) also reveals a sharp reduction in conductivity values after 30 min of hydration. This can be attributed to the consumption of the number of ions presented as a result of interaction between $Ca(OH)_2$ and the agglomerated sol of SF to form $Ca(OH)_2$-rich C-S-H [24]. With increasing duration of hydration, a sequence of interaction between SF grains and the initially formed $Ca(OH)_2$-rich C-S-H coating takes place, leading to a further decrease in the $Ca(OH)_2$ content of the initially formed C-S-H. The C-S-H is thus produced as a result of hydration interaction between the initially formed hydrates and the unhydrated parts of SF grains [24], i.e., the small particles of SF act as nucleation sites for the final C-S-H products. This reflects the low siemens values of all specimens under investigation after 3 h of hydration.

Figs. (3) and (4) show the effect of molar $Ca(OH)_2$/SF ratio on the electrical conductivity of the various $Ca(OH)_2$–SF pastes. It is clear that the intensity of the conductivity peak is affected by the molar $Ca(OH)_2$/silica ratio of the paste; it has the lowest siemens value for the paste made of mix IIa ($Ca(OH)_2$/silica = 0.80) while the peak obtained for the paste of mix IIb ($Ca(OH)_2$/silica = 1.0) has the highest intensity. Therefore, the molar $Ca(OH)_2$/silica ratio of 1.0 represents the maximum rate of initial hydrolysis of $Ca(OH)_2$–SF blend. On the other hand, the heights of the conductivity maxima for mixes IIc and IId having the molar $Ca(OH)_2$/silica ratio of 1.30 and 1.70, respectively, are lower than that of mix IIb and higher than that of mix IIa. This result can be explained in the light of the decreased degree of SF–gel formation as a result of coating of SF grains with the excess calcium hydroxide of blends IIc and IId.

Figs. (3b) and (4b) illustrate a similar temperature effect on the electrical conductivity values of the different $Ca(OH)_2$–SF pastes as reported in Figs. (1b) and (2b).

It is clear from Fig. (4) that all the conductograms obtained using W/S = 1.20 are characterized by higher peak intensity than the corresponding conductograms made with W/S = 1.0 (Fig. 3). Obviously, the increase of W/S ratio

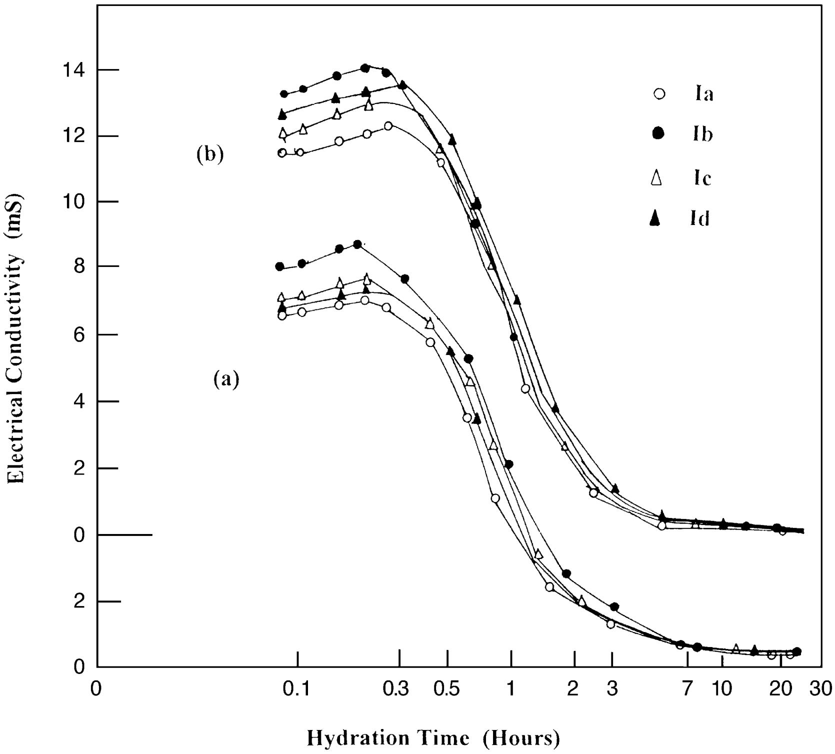

Fig. 3. Electrical conductivity–time curves of $Ca(OH)_2$–SF pastes of mixes IIa, IIb, IIc, and IId using W/S ratio of 1.00 at two temperatures (a) 25 and (b) 45 °C.

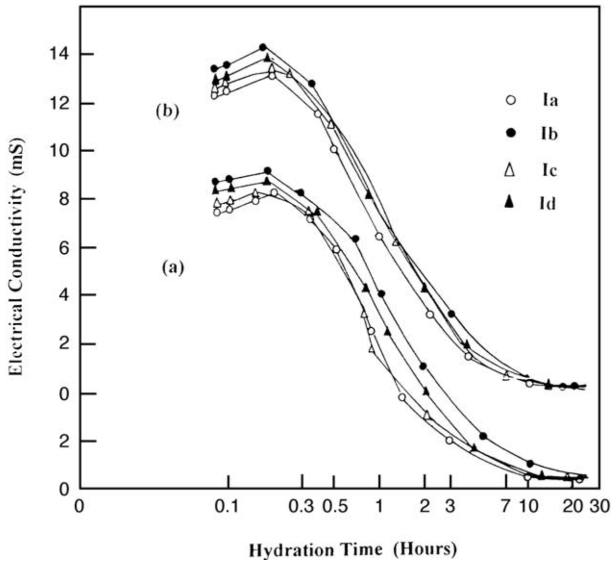

Fig. 4. Electrical conductivity–time curves of $Ca(OH)_2$–SF pastes of mixes IIa, IIb, IIc, and IId using W/S ratio of 1.20 at two temperatures (a) 25 and (b) 45 °C.

leads to an increase in both of the initial hydrolysis of $Ca(OH)_2$ and SF as well as the mobility of ions.

3.2. Rheological properties

It was well established that fresh cement pastes are initially a thick suspension of the cement particles in the mixing water. The structure of this suspension depends upon the water/cement (W/C) ratio, the particle size distribution of the cement, the interparticle forces and attraction of the water to solid surfaces, which in turn depends upon surface charges, ionic species, concentration in solution, and sorption from solution. In dilute suspension, cement particles normally will flocculate, forming separate clusters of particles, namely floccules, which settle rapidly. In cement pastes, the separate floccules in the static state merge into a single continuous large floc; there are aggregations of higher than average particle concentration between which are water-filled interstices. Within these aggregations, the particles tend to have smaller interparticle separations corresponding to minimum potential energy configurations; this represents the flocculent state as designated by Powers [25].

During mixing, the cement particles tend instead to become more uniformly dispersed in the water. There is a continuous breaking down of the structure during mixing; this is the origin of thixotropic or shear-thinning behavior of cement pastes.

3.2.1. OPC–SF system

Rheological measurements were carried out for the OPC–SF mixes having the weight ratios of 90:10, 80:20, 70:30, and 50:50; these mixes are designated as Ia, Ib, Ic, and Id, respectively. The W/S ratios used were 0.55, 0.60, 0.70, and 0.80. Figs. (5) and (6) show representative sets of shear rate–shear stress curves (flow curves) obtained for all specimens at the W/S ratio of 0.60 and 0.80, respectively. The first cycles of all samples show the behavior of thixotropy for the pastes made using the two selected W/S ratios (0.60 and 0.80), except those of samples Ia and Ib made using a W/S ratio of 0.80, which exhibit a mixed behavior (cf. Fig. 6). In the second and third cycles, the mixed behavior becomes more dominant for most of the pastes, except those for the pastes made of mixes Ia and Ib

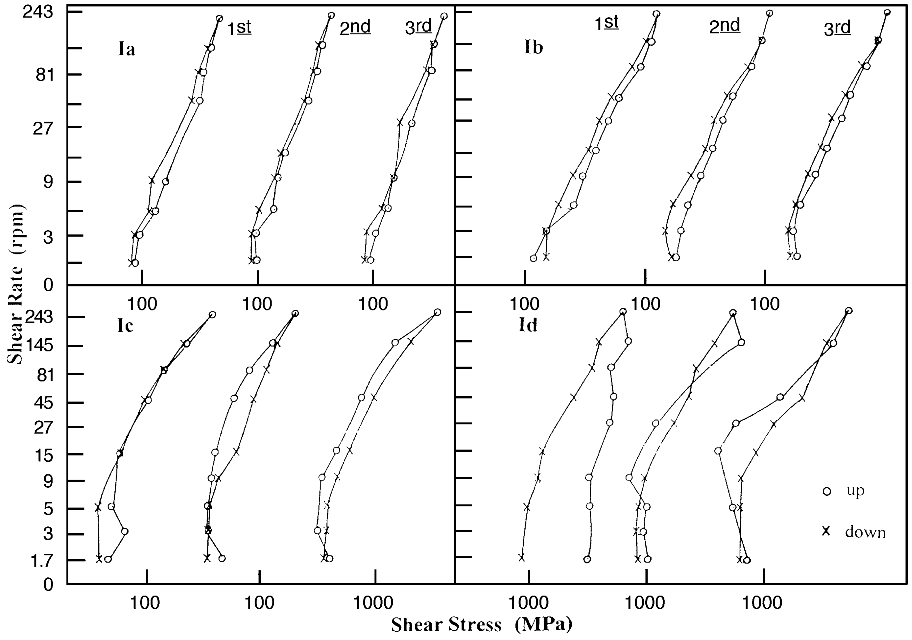

Fig. 5. Flow curves of OPC–SF pastes of mixes Ia, Ib, Ic, and Id using W/S ratio of 0.60.

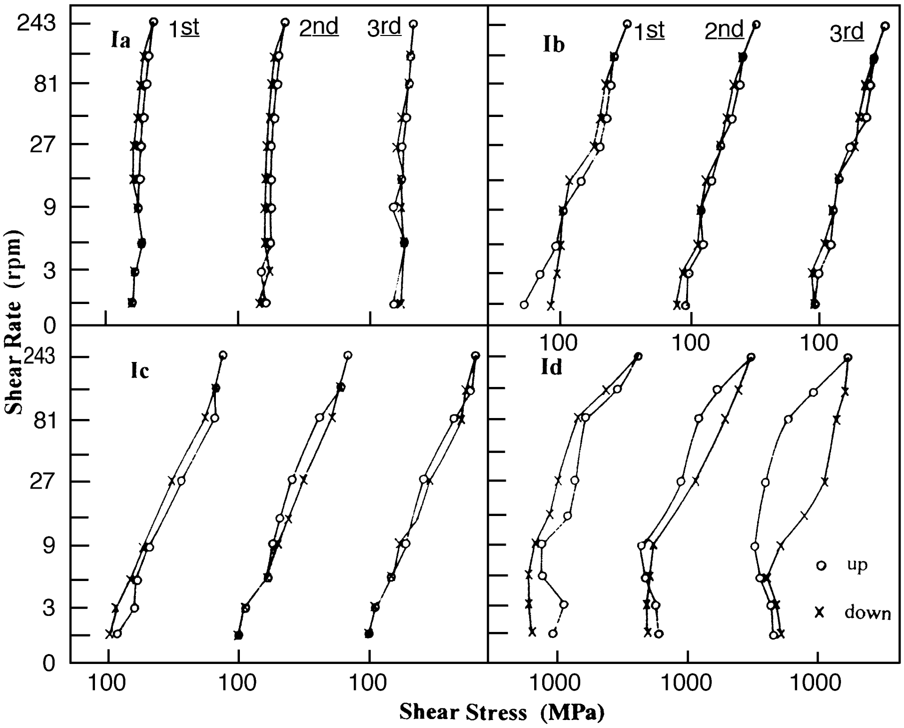

Fig. 6. Flow curves of OPC–SF pastes of mixes Ia, Ib, Ic, and Id using W/S ratio of 0.80.

using a W/S ratio of 0.60, which show a thixotropic behavior. Evidently, the yield value and the hysteresis area of the three cycles are changed with the variations in the SF content in the pastes from Ia to Id. The hysteresis area increases with increasing SF content of the paste, indicating a notable structure breakdown; this effect is related to ettringite–monosulfate transformation in addition to the retardation of Portland cement hydration as a result of coating cement grains by the fine particles of SF. The hysteresis areas for all specimens decrease as W/S ratios increase. On the other hand, the yield values increase for samples having a low SF content (Ia and Ib) and decrease for specimens having a high SF content (Ic and Id). This thixotropic character is unchanged in both of the second and third cycles for mixes having relatively low SF content (Ia and Ib); whereas mixed behavior rheographs are obtained for mixes having relatively high SF contents (Ic and Id).

To explain these rheological results, it would be more convenient to clarify the hydration reaction of the different mixes (Ia–Id) at early ages. Thus, when OPC–SF mixture is mixed with water, it appears that the solution immediately becomes supersaturated with respect to hydrated calcium silicates and aluminates as well as calcium hydroxide. From this supersaturated solution, the products of hydration precipitate as a gel around the unhydrated particles. After these initial solution reactions, further hydration proceeds by diffusion through the gel. Also, the sudden conversion of SF particles into a "sol" or a "gel," which then agglomerates [23] and reacts with the liberated $Ca(OH)_2$ to form C-S-H. As the hydration process proceeds, more interactions occur between the SF grains and the initial C-S-H coating [24].

Generally, the hydration products of OPC–SF pastes possess fiber-like and/or laminar habit. Such particles may form a loosely "cardhouse," i.e., edge to edge, structure, held together by low intermolecular forces; this is the intrinsic cause of thixotropy. Even small forces can interrupt edge-to-edge bonds, while they are recovered by random collision again. Thus, a changing equilibrium determined by the contact buildup and breakdown of the preformed structure is obvious, while these in turn are affected by external forces such as the thickness of the "lubricant" around particles, the presence of admixture (SF), and most important the shear stress in the suspension.

Obviously, in the various OPC–SF mixes, the first cycles show mainly a thixotropic behavior at the W/S ratio of 0.60 (Fig. 5); this indicates that at the early hydration ages and cycle time, structure buildup is slow compared to the rate of breakdown, also this thixotropic behavior is a result of the presence of forces between the cement and SF particles that are insufficiently strong to hold the system together. Such forces can be easily broken down by small shear stress. These forces can be attributed to the hydration products formed by: (i) the hydration of the main components of cement especially tricalcium aluminate that is rapidly hydrated yielding ettringite and/or monosulfate in the presence of gypsum and (ii) the interaction of SF with the liberated $Ca(OH)_2$ with the new formation of C-S-H.

The second and third cycles of the mixes Ia and Ib show thixotropic behavior with increase in the yield value and a

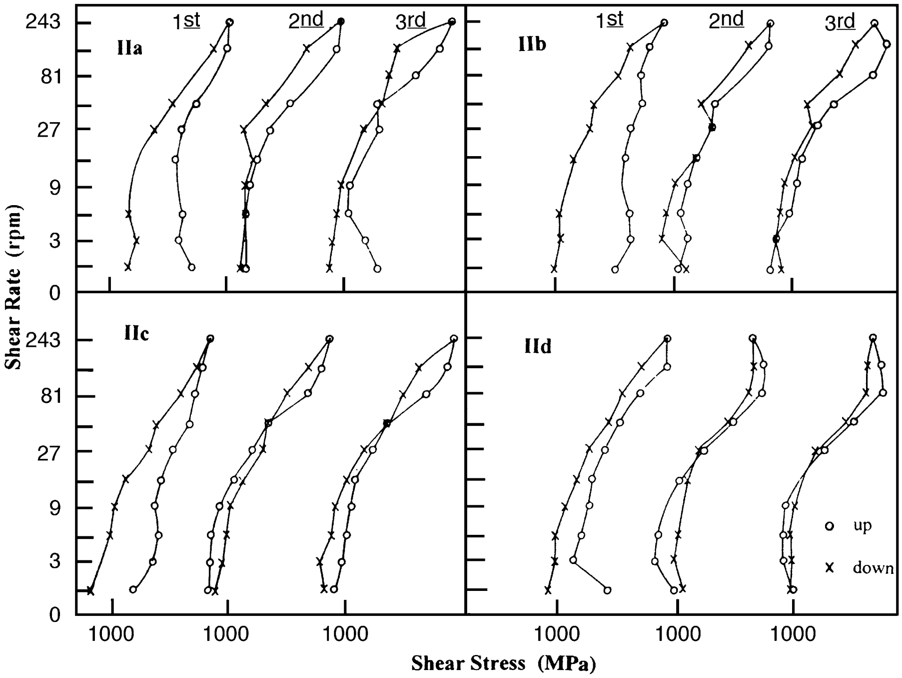

Fig. 7. Flow curves of $Ca(OH)_2$–SF pastes of mixes IIa, IIb, IIc, and IId using W/S ratio of 0.90.

slight change in the hysteresis area while the other mixes Ic and Id show a mixed behavior (thixotropic–antithixotropic) with a decrease in the yield value and the hysteresis area as well. The mixed character probably represents intermediate stages where the rate of buildup and breakdown are comparable [26].

Fig. (6) shows the flow curves of cement pastes containing different amounts of SF at W/S ratio 0.80. Clearly, the three successive cycles of all mentioned pastes show a mixed behavior, except the first cycles of Ic and Id pastes that show a thixotropic character. It can be concluded that as the W/S ratio increases, the rate of buildup competes with the rate of breakdown.

3.2.2. $Ca(OH)_2$–SF system

Rheological measurements were also carried out on four solid mixtures, prepared at $Ca(OH)_2$/SF molar ratios of 0.80, 1.00, 1.30, and 1.70. These mixes are designated as

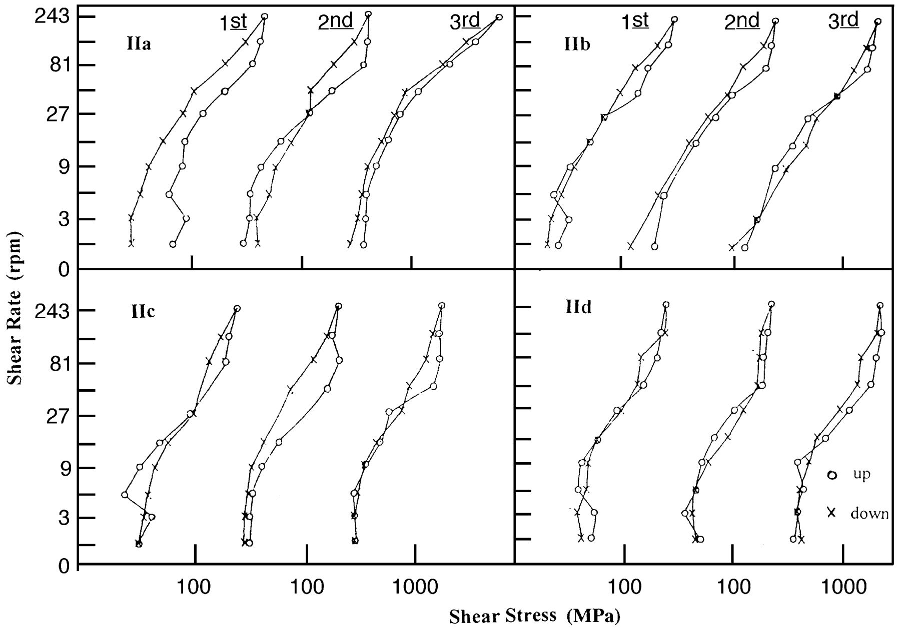

Fig. 8. Flow curves of $Ca(OH)_2$–SF pastes of mixes IIa, IIb, IIc, and IId using W/S ratio of 1.10.

IIa, IIb, IIc, and IId, respectively. Each dry mixture was mixed with deionized water at W/S weight ratio of 0.80, 0.90, 1.00, 1.10, and 1.20, respectively, and rheological measurements were done for all specimens as described earlier in this study.

The rheological studies obtained for all the pastes prepared by the W/S ratios 0.90 and 1.10 were taken as representatives for all $Ca(OH)_2$–SF pastes investigated; the results are shown in Figs. (7) and (8), respectively.

The flow curves obtained indicate that the first cycles of all specimens have a thixotropic character with large hysteresis loops at a W/S ratio of 0.90, while their behavior changed mainly to a mixed character (thixotropic–antithixotropic) at a W/S ratio of 1.10 with a noticeable change in the hysteresis loop (cf. Fig. 8); this result is mainly due to the increase in both the initial hydrolysis of $Ca(OH)_2$ and SF as well as the mobility of ions.

Both the second and third cycles of all pastes at the two W/S ratios show mainly mixed behavior and occasionally with some thixotropic and reversible behaviors. In addition, for the same pastes the hysteresis areas and the yield values are decreased as the W/S ratio increased; this is due to the decrease of the breakdown rate and therefore a decrease in the thixotropic extent.

Evidently, the results of Figs. (7) and (8) showed a marked narrowing in the width of the hysteresis loops with increasing the molar $Ca(OH)_2$/SF ratio of the solid mixture for all cycles; this effect is mainly associated with an increase in the buildup rate.

4. Conclusions

The main conclusions derived from the results of the rheological and electrical conductivity studies for OPC–SF and $Ca(OH)_2$–SF mixes under investigation may be summarized as follows:

1. The conductograms of all the OPC–SF blends show two conductivity peaks, the first peak is attributed to the initial hydrolysis of the OPC constituents, while the second transient maximum is explained by the ettringite–monosulfate transformation.

2. The second conductivity peak is shifted towards a shorter time of hydration with increasing SF content of the OPC–SF blends; similar effect was also observed with increasing hydration temperature.

3. The results of rheological properties indicate that the hysteresis area increases with increasing SF content of the OPC–SF pastes, indicating a notable structure breakdown (thixotropic behavior). This result is related to the consumption of free $Ca(OH)_2$ via interaction with SF, leading to the acceleration of ettringite–monosulfate transformation. This reveals the shift of the second conductivity peak towards a shorter curing time.

4. The hysteresis areas for all OPC–SF specimens decrease as the W/S ratio increases as obtained from rheological studies; this result is mainly attributed to the fact that the ettringite is still existing with a sufficient stability for a longer hydration period for the pastes made with higher water contents. This effect is also associated with the shift of the second conductivity peak towards a longer hydration time.

5. For mixes made with a W/S ratio of 0.60, the thixotropic character is unchanged in both the second and third cycles for mixes made with lower SF contents, while mixes having higher SF contents showed mainly a mixed behavior.

6. For the pastes made with the higher W/S ratio (W/S = 0.80), all mixes made with various SF contents showed a mixed behavior; a result that is mainly related to the delayed ettringite–monosulfate transformation.

7. All the conductograms obtained for the $Ca(OH)_2$–SF pastes are characterized by one conductivity maximum. The intensity of the maximum is affected by both the molar $Ca(OH)_2$/silica ratio and W/S ratio. This conductivity peak is a consequence of the initial hydrolysis of $Ca(OH)_2$ and also the sudden conversion of SF particles into a “sol” or a “gel.”

8. For the pastes made of $Ca(OH)_2$ and SF, it was found that upon increasing the W/S ratio of the paste, the thixotropic behavior of the first cycles is changed to a mixed behavior with a noticeable narrowing in the hysteresis loops; this result is mainly due to the increase in both of the initial hydrolysis of $Ca(OH)_2$ and SF as well as the mobility of ions. This effect is accompanied by an increase in the peak intensities of conductograms obtained for the pastes made by using a higher W/S ratio.

9. The increase of the molar $Ca(OH)_2$/SF ratio in the mixes is almost accompanied by a marked narrowing in the hysteresis loops of the flow curves indicating an increase in the antithixotropic character. The $Ca(OH)_2$-rich mixes (IIa and IIb) possess an excess free $Ca(OH)_2$ that increase the stability of the formed hydrates, mainly as $Ca(OH)_2$-rich calcium silicates.

References

[1] W.J. McCarter, A.B. Afshar, Some aspect of the electrical properties of cement pastes, J. Mater. Sci. Lett. 4 (1984) 1083.

[2] F.D. Tamas, Electrical conductivity of cement pastes, Cem. Concr. Res. 12 (1982) 115.

[3] W.J. McCarter, P.N. Curran, The electrical response characteristics of setting cement paste, Mag. Concr. Res. 36 (126) (1984) 42.

[4] F.D. Tamas, E. Farkas, M. Voros, D.M. Roy, Low frequency electrical conductivity of cement, clinker and clinker mineral pastes, Cem. Concr. Res. 17 (1987) 340.

[5] M. Saad, S.A. Abo-El-Enein, G.B. Hanna, M.F. Kotkata, Effect of temperature on physical and mechanical properties of concrete containing silica fume, Cem. Concr. Res. 26 (5) (1996) 669.

[6] M. Saad, S.A. Abo-El-Enein, G.B. Hanna, M.F. Kotkata, Effect of silica fume on the phase composition and microstructure of thermally treated concrete, Cem. Concr. Res. 26 (10) (1996) 1469.

[7] S.A. Abo-El-Enein, M.F. Kotkata, G.B. Hanna, M. Saad, M.M. Abd El Razek, Electrical conductivity of concrete containing silica fume, Cem. Concr. Res. 25 (8) (1995) 1615.

[8] L. Kucharska, M. Moczko, Influence of silica fume on the rheological properties of the matrixes of high performance concrete, Adv. Cem. Res. 6 (24) (1994) 139.

[9] D.M. Roy, K.M. Parker, Microstructure and properties of granulated slag–portland cement blends at normal and elevated temperatures, Proc. CANMET/ACI First Int. Conf. Use Fly Ash, Silica Fume, Slag Other Miner. By-Product Concr. Publ. SP-79 (1983) 397.

[10] J. Struble, L.L. Wei-Guo, rheological changes associated with setting of cement pastes, Adv. Cem. Based Mater. 2 (6) (1995) 224.

[11] S. Basma, L. Sarkar, Shondeep, Influence of different alkali combinations on the rheology of cements, J. World Cem. 28 (4) (1997) 110.

[12] R. Shaughnessy, P.E. Clark, The rheological behaviour of fresh cement pastes, Cem. Concr. Res. 18 (1998) 327.

[13] P. Billberg, Effect of mineral and chemical admixtures on fine mortar rheology, Am. Concr. Inst. SP-173 (1997) 301.

[14] O. Ludmilla, P. Adriano, Rheological and hydration properties of a high strength gypsum-free cement, Proc. Int. Congr. Chem. Cem. 10th, 2 (1997) 4–8.

[15] D. Peter, H.-W. Chai, Testing of binders for high performance concrete, J. Cem. Concr. Res. 27 (8) (1997) 1141.

[16] I. Ivanov, T. Roshavelov, The effect of condensed silica fume on rheological behaviour of cement pastes, Rheol. Fresh Cem. Concr. Proc. Int. Conf. (1990) 23–26.

[17] C. Younshik, A. Kiyoshi, T. Takaaki, D. Masaki, Rheological properties of cement–slag–silica fume pastes, Gypsum Lime 236 (1992) 12.

[18] M. Deng, M. Tang, Formation and expansion of ettringite crystals, Cem. Concr. Res. 24 (1994) 119.

[19] F.I. El-Hosiny, S.A. Abo-El-Enein, Z.A. Abou-Gamra, S.M.A. El-Gamal, Physicochemical and mechanical characteristics of autoclaved portland cement clinker, Silic. Ind. 65 (1–2) (2000) 19.

[20] Th.M. Salem, Sh.M. Ragai, Electrical conductivity of granulated slag–cement kiln dust–silica fume pastes at different porosities, Cem. Concr. Res. 31 (2001) 781.

[21] M. Saad Morsy, S.A. Abo-El-Enein, G.B. Hanna, Microstructure and hydration characteristics of artificial pozzolana–cement pastes containing burnt kaolinite clay, Cem. Concr. Res. 27 (9) (1997) 1307.

[22] E. Tkalcec, J. Zellic, Influence of amorphous silica (silica dust) on the properties of portland cement mortar, Zem.–Kalk–Gips 40 (1987) 574.

[23] M.W. Grutzeck, D.M. Roy, D. Wolf-Confer, Mechanism of hydration of portland cement composition containing ferrosilicon dust, 4th Int. Conf. Cem. Microsc., March 28–April 1, Las Vegas, USA (1982) 193.

[24] S.A. Abo-El-Enein, Z.M. Abou-Gamra, F.I. El-Hosiny, S.M.A. El-Gamal, Characteristics of $Ca(OH)_2$–silica fume mixtures, J. Therm. Anal. 46 (1996) 275.

[25] T.C. Powers, Rheology of Freshly Mixed Concrete, The Properties of Fresh Concrete, Wiley, New York, 1968.

[26] P.F.G. Banfill, D.C. Saunders, Viscometric examination of cement pastes, Cem. Concr. Res. 11 (1981) 363.